# The 3-Zones Extended Coherent Flame Model (Ecfm3z) for Computing Premixed/Diffusion Combustion

O. Colin, A. Benkenida

*Oil & Gas Science and Technology – Rev. IFP*, Vol. 59 (2004), No. 6, pp. 593-609


# The 3-Zones Extended Coherent Flame Model (ECFM3Z) for Computing Premixed/Diffusion Combustion

O. Colin[1] and A. Benkenida[1]

*Institut français du pétrole, Direction Techniques d'applications énergétiques*
*1 et 4, avenue de Bois-Préau, 92852 Rueil-Malmaison Cedex - France*
*e-mail: olivier.colin@ifp.fr - adlene.benkenida@ifp.fr*

**Résumé — Le modèle ECFM3Z *(3-Zones Extended Coherent Flame Model)* pour le calcul de la combustion par flammes de prémélange et flammes de diffusion** — Le modèle ECFM *(Extended Coherent Flame Model)* (Colin *et al.*, 2003), développé dans le but de modéliser la combustion de mélanges parfaitement ou partiellement homogènes, est adapté à la simulation de la combustion par flammes de diffusion (combustion se produisant dans une zone de réaction mince séparant le carburant de l'air) rencontrée en moteur Diesel par exemple. Le modèle ECFM est basé, d'une part, sur la résolution d'une équation de transport de la densité de surface de flamme prenant en considération le plissement du front de flamme engendré par les effets turbulents, et d'autre part, sur une méthode de conditionnement assurant une reconstruction précise des propriétés locales des gaz frais et des gaz brûlés, même dans des cas très fortement stratifiés. Ce modèle a été utilisé avec succès dans les calculs de moteurs essence (Duclos *et al.*, 1996 ; Duclos et Zolver, 1998 ; Lafossas *et al.*, 2002 ; Henriot *et al.*, 2003 ; Kleemann *et al.*, 2003). Afin d'adapter le modèle à la combustion par flammes de diffusion, une description de l'évolution de l'état du mélange a été ajoutée. Cette description consiste à découper tout volume de contrôle (typiquement une maille de la grille de calcul 3D) en trois zones de mélange : une zone de carburant pur, une zone d'air pur (et d'éventuels gaz résiduels) et une zone dans laquelle le carburant et l'air sont mélangés. C'est dans cette zone (appelée zone mélangée) que le modèle de combustion ECFM est appliqué. L'évolution de l'état du mélange est gérée par un modèle phénoménologique assurant le mélange progressif du carburant pur et de l'air pur (c'est-à-dire, le passage des deux zones non mélangées vers la zone mélangée). ECFM3Z est couplé avec le modèle d'auto-inflammation développé par Colin *et al.* (2004). Il a déjà été brièvement décrit dans une étude consacrée à la comparaison entre mesures expérimentales et calculs sur un moteur Diesel (Béard *et al.*, 2003). Cette étude est consacrée à une présentation détaillée du modèle ECFM3Z. Son comportement est analysé à travers une variation de la durée d'injection et du délai d'auto-inflammation en moteur Diesel. Les résultats montrent clairement que le modèle est capable de reproduire l'importance relative de l'auto-inflammation et des flammes de diffusion sur le dégagement de chaleur en fonction du point de fonctionnement moteur considéré.

***Abstract* — *The 3-Zones Extended Coherent Flame Model (ECFM3Z) for Computing Premixed/Diffusion Combustion*** — *The Extended Coherent Flame Model of Colin* et al. *(2003) developed to model combustion in perfectly or partially mixed mixtures is adapted to also account for unmixed combustion. The ECFM model is based on a flame surface density equation which takes into*

*account the wrinkling of the flame front surface by turbulent eddies and a conditioning averaging technique which allows precise reconstruction of local properties in fresh and burned gases even in the case of high levels of local fuel stratification. This model has been used with success in gasoline engines (Duclos* et al.*, 1996; Duclos and Zolver, 1998; Lafossas* et al.*, 2002; Henriot* et al.*, 2003; Kleemann* et al.*, 2003). In order to adapt the model to unmixed combustion for Diesel application, a description of the mixing state has been added. It is represented by three mixing zones: a pure fuel zone, a pure air plus possible residual gases zone and a mixed zone in which the ECFM combustion model is applied. A mixing model is presented which allows progressive mixing of the initially unmixed fuel and air. This new combustion model, called ECFM3Z (3-Zones Extended Coherent Flame Model), can therefore be seen as a simplified CMC (Conditional Moment Closure) type model where the mixture fraction space would be discretized by only three points. The conditioning technique is extended to the three mixing zones and allows to reconstruct, like in the ECFM model, the gas properties in the unburned and burned gases of the mixed zone. Application of the model to internal combustion engine calculations implies the necessity of auto-ignition modelling coupled to premixed and diffusion flames description. Auto-ignition is modelled following (Colin* et al.*, 2004), while the premixed turbulent flame description is given by the ECFM. The diffusion flame is now accounted for thanks to the three zones mixing structure which represents phenomenologically the diffusion of fuel and air towards the reactive layer, that is the mixed zone. The ECFM3Z combustion model has already been presented (Béard* et al.*, 2003) in a comparative work between Diesel experiments and corresponding calculations covering different engine operating points. Here, the model is presented in all its details and its behavior is analysed when the relative duration of injection and auto-ignition delay are varied in a direct injection Diesel engine. It is shown that the model is able to reproduce the relative importance of auto-ignition and diffusion flame on the total heat release, depending on the engine operating point considered.*

## INTRODUCTION

International regulations are imposing in recent years more and more stringent limitations on pollutant emissions and consumption for combustion devices. Automotive industry uses two types of Internal Combustion Engine (ICE): the Spark Ignition (SI) gasoline engine and the Compression Ignition (CI) Diesel engine. However, these concepts will probably fail in complying with future environmental norms. This has lead car manufacturers and laboratories to develop new combustion systems for ICE like CAI (Compression Auto-Ignition) for gasoline or HCCI (Homogenous Charge Compression Ignition) for Diesel. At the present state of research, these new combustion modes do not allow to reach high specific powers like classical SI and CI engines, although they permit very low pollutant emissions. Therefore, future generations of engines will probably use both SI and CAI concepts for gasoline fuel or HCCI and CI concepts for Diesel fuel. CAI and HCCI will be used for low to medium load operating points while the engine will switch to SI or CI for high load operation.

Computational Fluid Dynamics (CFD) techniques used to solve the Reynolds Averaged Navier-Stokes (RANS) equations have become nowadays a useful tool for engine manufacturers. First, they allow a better understanding of how combustion takes place in new combustion concepts. Second, rapid and low cost testing of different chamber geometries and concepts can be performed in order to design the final product.

Classically, RANS engine combustion models have been clearly divided into premixed combustion models for SI engines and nonpremixed combustion models for Diesel engines. This separation becomes less and less justified for many reasons. This can be understood by defining the three main combustion modes encountered in industrial devices. The first two modes are of the premixed type. A premixed charge of air and fuel can auto-ignite after an auto-ignition delay essentially controlled by temperature, pressure, fuel/air equivalence ratio and residual gases fraction. This type of combustion, from now on called AI, controls the beginning of combustion in Diesel engines and can also be found in SI engines as a undesirable combustion commonly called knock. The second premixed combustion mode is the premixed Propagation Flame (PF) used in SI engines. In this case the combustion chamber is filled with a premixed charge of fuel and air. A spark plug generates a small spherical propagation flame between the electrodes which afterwards propagates in the combustion chamber until it has totally consumed the premixed fresh charge. The third combustion mode is the non-premixed combustion, also called Diffusion Flame (DF). Here, fuel and air are separated by a thin reaction zone in which burned gases are formed. As a first approximation, the chemical time in the reactive zone is usually considered much smaller than the diffusion time involved in the diffusion of fuel and air towards the flame region. This is why this combustion mode is also called mixing controlled combustion. This type of combustion follows combustion by auto-ignition in Diesel engines.

The above description shows that the combustion process taking place in Diesel engines cannot be considered solely as non-premixed: the onset of combustion is controlled by partially premixed AI which is responsible for the rapid initial pressure rise in the chamber. This type of combustion can represent an important part of the total heat release in the cycle, depending on the engine operation point. Also, the new combustion concepts such as CAI or HCCI are not clearly identified as premixed or nonpremixed combustion. For both concepts AI is responsible for the start of combustion, but afterwards, experiments have shown that the charge is not perfectly mixed during combustion (Docquier, 2003). It is therefore possible that combustion proceeds simultaneously through PF and DF.

This observation has lead to the development of unified combustion models able to account for all types of combustion simultaneously occurring inside the chamber, avoiding the problem of choosing the model before hand. Abraham *et al.* (1985) and Kong *et al.* (1995) proposed an extended characteristic-time model which accounts for chemical and turbulent time scales simultaneously: in a classical Diesel engine, combustion is first controlled by the chemical time (AI period), and then by the turbulent time (DF combustion). Even if premixed and nonpremixed combustion are taken into account in this model, the unmixedness of species within a computational cell is only represented by a mixing time-scale, which does not allow to represent the history of mixing (the mixed part of the mixture increases with time). As a consequence, the transition between chemically controlled and mixing controlled combustion needs to be monitored by an empirical function. This model does not account for PF combustion, it is therefore restricted to Diesel type applications. The two zone flamelet model (Chen *et al.*, 2000) proposes a description of the incomplete mixing within a computational cell by separating unburned gases in two zones: a segregate region which contains unmixed fuel and air, and a fully mixed region which contains the unburned mixed fuel and air. The gases of the mixed region are consumed by AI and PF. Unlike models based on a mixing time, this model correctly represents the initial mixing of unburned fuel and air which leads to the formation of a premixed charge that will rapidly auto-ignite. In a second phase, the chemical time (represented by the premixed flame time scale) becomes smaller than the mixing time, and a non-premixed combustion is recovered. Although the mixed zone is represented, the volume occupied by this region is roughly estimated in this model. This does not allow a precise computation of species mass fractions, temperature and density in this region. As a consequence, the unburned gases properties like the laminar flame speed, or the auto-ignition delay time are only approximately estimated. In the same way, it becomes difficult to perform post-flame kinetics in the burned gases as properties in this zone are not precisely defined as well.

During the last decade, new approaches were developed with the aim of representing the diffusion flame and auto-ignition in a more rigorous manner. The flamelet approach was developed by Peters *et al.* (Peters, 1986; Pitch, 1995). In this model, the reaction rate is tabulated for a laminar diffusion flame in mixture fraction space for different values of the scalar dissipation rate. The mean reaction rate is then obtained by integrating this laminar reaction rate over all possible values of the mixture fraction using a presumed pdf (probability density function) for the mixture fraction and the instantaneous scalar dissipation rate observed in the flow field. This model has the advantage of including both finite rate chemistry and the influence of the local mixture fraction gradients imposed by the flow field. More recently, the EPFM (Eulerian Particle Flamelet Model) (Pitch, 1998; Hasse *et al.*, 2000), allowed to consider simultaneously a couple of unsteady flamelets solved in a dedicated flamelet code, while in parallel, Navier-Stokes equations were solved in a CFD code. This model allows to represent AI and DF, but mixing and combustion, which are very local phenomena in a piston engine, are represented in an averaged way since flamelets are based on the averaged properties over entire parts of the domain. This model does not account for PF combustion and the CPU cost increases rapidly with the number of flamelets involved. In the CMC (Conditional Moment Closure) approach (Klimenko and Yu, 1990; Bilger, 1993), the mixture fraction $Z$ is not represented solely by its mean value and fluctuation like in most models, but the $Z$-space is discretised, and combustion and mixing processes are solved conditioned for different values of $Z$. This approach is therefore very promising but its CPU cost in an industrial context remains for the moment prohibitive. PF combustion can be represented by this approach, but in this case, the reaction progress (fraction of unburned gases) dimension must be added, making the calculation even more CPU consuming. In the transported pdf approach (see for instance (Veynante, 2000) for a review of these models), no assumption is made on the shape of the mixture fraction pdf. The pdf is directly transported using Monte-Carlo methods. Although these methods are complex to develop and induce an important CPU cost, calculations on ICE are now being performed with such models (Zhang, 2004).

More recently, new approaches were proposed to model auto-ignition and diffusion flames by considering only the dimensions of mixing, represented by the mean mixture fraction and its fluctuation, and the dimension of advancement of reaction, represented by the mean progress variable and its fluctuation (or equivalently by the flame surface density). These approaches are much less CPU consuming than CMC or EPFM models although they include realistic physics as they also rely on flamelet libraries. Flame surface density models, the PCM model and the model presented in this paper, ECFM3Z, belong to this type of approaches. The flame surface density approach was

first proposed in the context of diffusion flames in the pioneer work of Marble and Broadwell (1977). An exact balance equation for the flame surface density was proposed (Van Kalmthout, 1996) for diffusion flames. More recently, this approach has been extended by considering a generalised flame surface density including all possible values of the mixture fraction, with reaction rates per unit of flame surface given by a library of transient diffusion flames (Tap, 2004). The Presumed Conditional Moment (PCM) model (Vervish, 2004) is a simplified version of the CMC approach where conditional moments of the progress variable are presumed and the conditional reaction rates and species mass fractions are given by the FPI (Flame Prolongation of ILDM) approach (Gicquel, 2004) which is based on tabulations of premixed and unpremixed stationnary flamelets.

The ECFM (Colin *et al.*, 2003) is a version of the flame surface density approach (Candel and Poinsot, 1990; Boudier *et al.*, 1992), which allows the simulation of the two premixed combustion modes, PF combustion in SI engines as well as knock (AI) and pollutant formation, even in highly stratified cases. Based on this model, the unified Diesel/gasoline combustion model ECFM3Z was briefly presented in (Béard *et al.*, 2003). In this model, the unburned/burned gas zones description of the ECFM model is kept, as well as the premixed flame description based on the flame surface density equation. In order to account for DF and mixing processes, each computational cell is split into three mixing zones: a pure fuel zone, a pure air plus possible residual gases (EGR) zone and a mixed zone, as schematically presented in Figure 1. This structure allows to account for the three main combustion modes (AI, PF and DF) encountered in most combustion devices.

The aim of this paper is to describe the ECFM3Z model in detail. In the first part, we introduce the principle of the model based on its three zones structure. Then the structure of the model is presented in detail. It is based on two dimensions classically used for solving combustion problems: the mixing state (mixture fraction description) and the reaction progress (progress variable description). The way the three main combustion modes are computed is then explored and it is shown how the pollutant formation is accounted for in the burned gases. Finally, the behaviour of the model is analysed over two different operation points of a conventional Diesel engine.

## 1 PRINCIPLE OF THE ECFM3Z MODEL

In the ECFM3Z combustion model, the state of the gases mixture is defined in the 2D space (Z, $\tilde{c}$). It is simultaneously described in terms of mixing and progress of reaction as schematically represented in Figure 1.

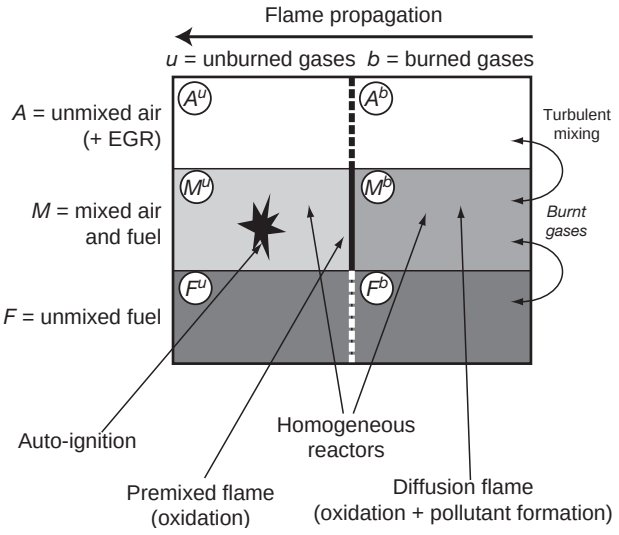


Figure 1

Schematic of the ECFM3Z model computational cell.

### 1.1 Mixing Description

According to the ECFM3Z zone splitting *(Fig. 1)*, each computational cell is divided into three mixing zones: the unmixed fuel zone (letter *F* in the figure), the mixed zone containing fuel, air and EGR (letter *M*), and the unmixed air + EGR zone (letter *A*). This structure can be seen as the representation of the Probability Density Function (PDF) of the mixture fraction variable *Z* by a three delta distribution:

$$P(Z) = a\delta(Z) + b\delta(Z - \overline{Z}^{M}) + c\delta(Z - 1) \qquad (1)$$

where $\overline{Z}^{M}$ is the average value of the mixture fraction in the mixed zone. Here, the mixture fraction is defined as the fuel tracer species $\widetilde{Y}_{TFu}$ defined latter in this paper.

The first delta function corresponds to the unmixed air region *A*, the second one to the mixed region *M* and the third one to the unmixed fuel region *F*. This structure can be seen as a simplified CMC approach where the discretisation in the *Z* space is performed by only three points. The mixing model presented in Section 2.3.1 allows to progressively transfer unmixed fuel and unmixed air into the mixed region.

In the unmixed fuel region *F* we assume the local fuel mass fraction is one only as a first step of modelling. In reality, the maximal fuel mass fraction encountered is given by the fuel mass fraction at saturation conditions around fuel droplets. As this mass fraction evolves with ambient pressure and temperature, it is a challenge to model it in the context of ICE. We leave this task for future development of the model.

### 1.2 Reaction Progress Description

As combustion can obviously not take place in regions *A* and *F*, it is only considered possible in region *M*. Combustion

calculations are thus conditioned in this zone according to the description directly taken from the ECFM model (Colin *et al.*, 2003). We consider two possible states for gases during combustion: the unburned gas zone and the burned gas zone corresponding to superscripts $u$ and $b$ in Figure 1. The amount of unburned/burned gases in the mixed zone $M$ is given by the progress variable $\tilde{c}$ which is equal to zero when the burned gas mass is zero, and equal to one when the total mass contained in the mixed zone has been burned. Burned gases of region $M^b$ have a temperature $T^b$ while the gases of the five other regions have the same temperature $T^u$. Therefore, even if regions $F^b$ and $A^b$ have the same superscript $b$, they do not correspond to burned gases but rather to unburned gases which will mix in region $M^b$.

### 1.3 Evolution of the *(Z,c)* Description During Combustion

In order to understand how the different zones evolve during combustion, we consider the case of a direct injection type combustion chamber. Initially, the chamber contains only pure air corresponding to region $A^u$. The liquid fuel spray injected in the chamber evaporates, and the gaseous fuel formed feeds region $F^u$. This way, fuel and air are initially entirely unmixed, that is, region $M$ is empty. This situation corresponds to case A in Figure 2. The mixing model allows to progressively transfer unmixed fuel and unmixed air in the mixed region $M^u$, corresponding to case B in Figure 2. As soon as region $M^u$ is formed, the auto-ignition delay time is computed in this zone, as described in Colin *et al.* (2004). If the auto-ignition delay is reached, the fresh gas mass in region $M^u$ is rapidly consumed. The burned gases formed are placed in region $M^b$, which leads to case C in the same figure.

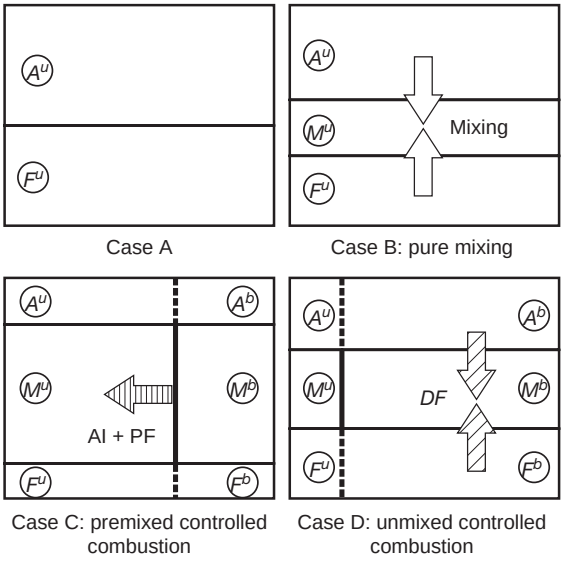


Figure 2

Evolution of the ECFM3Z zones during combustion.

Another possible way to start combustion is to create a premixed flame separating unburned and burned gases (as schematically represented in Figure 1) with a spark plug. As described in Duclos and Colin (2001) and Colin *et al.* (2003), the AKTIM (Arc and Kernel Tracking Ignition Model) spark plug ignition model allows to precisely compute the amount of flame surface deposited at spark timing. In this case, the ECFM model gives the evolution of the flame surface (by solving a transport equation for the flame surface density (Colin *et al.*, 2003)) that will consume the unburned gases of region $M^u$ and form the burned gases in region $M^b$, finally leading to the same situation C in Figure 2.

In the burned gases region $M^b$, the post-flame kinetics are computed, which include a simple Arrhenius model for the oxidation of possibly remaining fuel (in the case of very rich mixtures or DF combustion), the formation of NOx (Heywood, 1988), soot (Martinot *et al.*, 2001) and CO and chemical equilibrium (see Section 3.3) which allows to obtain a precise burned gases temperature as well as an estimation of pollutant species concentrations (NO, CO and soot).

In Diesel type applications, it is possible that even when combustion has begun in the mixed region (that is $\tilde{c} > 0$), the mass of unmixed fuel and air present in regions $F$ and $A$ is still important, corresponding schematically to case D in Figure 2. In this case, these unmixed gases continue to migrate into the mixed region. The fraction $\tilde{c}$ of the gases contained in region $F$ (respectively $A$), which corresponds to region $F^b$ (respectively $A^b$), mixes with the burned gases of region $M^b$. They are consumed afterwards by the post-flame kinetics in region $M^b$. As the mixing time is usually much larger than the chemical time involved in the burned gases of region $M^b$, this case represents combustion controlled by mixing, that is, diffusion flame (DF) combustion. The other fraction $(1 - \tilde{c})$ of these unmixed gases mixes with the unburned gases of region $M^u$. They are consumed afterwards by PF or AI. It is important to notice that gases contained in regions $F^u$ and $F^b$ (regions $A^u$ and $A^b$ respectively) have the same composition and the same temperature $T^u$, and only differ in their presumed location.

This schematic description of the combustion process with ECFM3Z shows that all combustion modes are simultaneously represented in this model. This allows application of the model to all types of combustion devices without the need to guess beforehand the type of combustion that will be encountered. In the following part we describe in detail how the different zones represented in Figure 1 are computed and how they exchange mass and energy.

## 2 THE 2D *(Z,c)* DESCRIPTION OF GASES STATE

In this section we explain how the quantities defined in the different zones of the ECFM3Z model are computed. We

start by defining the global species equations and the progress variable $\tilde{c}$, then we present the mixing model that computes unmixed species and deduce mixed species (this corresponds to gases description according to *Z*). Finally, we explain how the properties of the unburned and burned gases contained in the mixed zone are obtained (this corresponds to gases description according to $\tilde{c}$).

## 2.1 The Global Species Equations

In the ECFM3Z model, a transport equation is solved for the Favre average mass densities of chemical species fuel, $O_2$, $N_2$, NO, $CO_2$, CO, $H_2$, $H_2O$, O, H, N, OH and soot inside the computational cell containing the three mixing zones. Therefore, when "burned gases" are mentioned they include the real burned gases in the mixed zone (zone $M^b$ in Figure 1) plus a part of the unmixed fuel (zone $F^b$ in Figure 1) and air (zone $A^b$ in Figure 1). These equations are classically modeled as:

$$\frac{\partial \bar{\rho}\tilde{Y}_X}{\partial t}+\frac{\partial \bar{\rho}\tilde{u}_i\tilde{Y}_X}{\partial x_i}=\frac{\partial}{\partial x_i}\left(\left(\frac{\mu}{Sc}+\frac{\mu_t}{Sc_t}\right)\frac{\partial \tilde{Y}_X}{\partial x_i}\right)+\bar{\dot{\omega}}_x \quad (2)$$

where $\mu$ and $\mu_t$ are the laminar and turbulent viscosities respectively, and *Sc* and $Sc_t$ are the laminar and turbulent Schmidt numbers. $\bar{\dot{\omega}}_x$ is the average combustion source term and $\tilde{Y}_x$ is the average mass fraction of species *x*:

$$\tilde{Y}_x=\frac{\overline{m}_x}{\overline{m}}=\frac{\overline{m}_x/V}{\overline{m}/V}=\frac{\bar{\rho}_x}{\bar{\rho}} \quad (3)$$

*V* is the cell volume, $\bar{\rho}$ is the mean density and $\overline{m}=\bar{\rho}V$ is the cell mass.

The fuel is divided in two parts: the fuel present in the fresh gases $\tilde{Y}^u_{Fu}$, and the fuel present in the burned gases $\tilde{Y}^b_{Fu}$. This division is necessary to represent the fact that a part $\tilde{Y}^u_{Fu}$ of the fuel will be consumed by AI or PF, while the remaining fuel $\tilde{Y}^b_{Fu}$ will be consumed by a DF. The fuel transport equations are:

$$\begin{aligned}\frac{\partial \bar{\rho}\tilde{Y}^u_{Fu}}{\partial t}+\frac{\partial \bar{\rho}\tilde{u}_i\tilde{Y}^u_{Fu}}{\partial x_i}&=\frac{\partial}{\partial x_i}\left(\left(\frac{\mu}{Sc}+\frac{\mu_t}{Sc_t}\right)\frac{\partial \tilde{Y}^u_{Fu}}{\partial x_i}\right)+\bar{\rho}\tilde{\dot{S}}^u_{Fu}+\bar{\dot{\omega}}^u_{Fu}-\bar{\dot{\omega}}^{u\to b}_{Fu}\\ \frac{\partial \bar{\rho}\tilde{Y}^b_{Fu}}{\partial t}+\frac{\partial \bar{\rho}\tilde{u}_i\tilde{Y}^b_{Fu}}{\partial x_i}&=\frac{\partial}{\partial x_i}\left(\left(\frac{\mu}{Sc}+\frac{\mu_t}{Sc_t}\right)\frac{\partial \tilde{Y}^b_{Fu}}{\partial x_i}\right)+\bar{\rho}\tilde{\dot{S}}^b_{Fu}+\bar{\dot{\omega}}^b_{Fu}+\bar{\dot{\omega}}^{u\to b}_{Fu}\end{aligned} \quad (4)$$

During the evaporation of liquid fuel droplets, the gaseous fuel produced, $\tilde{\dot{S}}_{Fu}$, is distributed between unburned and burned fuel supposing the probability to find a droplet in the burned gases (resp. unburned gases) is $\tilde{c}$ (resp. $(1-\tilde{c})$):

$$\begin{aligned}\tilde{\dot{S}}^b_{Fu}&=\tilde{\dot{S}}_{Fu}\tilde{c}\\ \tilde{\dot{S}}^u_{Fu}&=\tilde{\dot{S}}_{Fu}(1-\tilde{c})\end{aligned} \quad (5)$$

In the case of local fuel/air (F/A) equivalence ratios higher than stoichiometry, there is not enough oxygen in the fresh gases to completely oxidize the fuel. Therefore a part of the fuel contained in region $M^u$ and going through the PF, or consumed by AI, is not oxidized and ends up in the burned gases region $M^b$, where it can be post-oxidized. In the same way, the unburned fuel contained in region $F^u$ is not oxidized at all when AI or PF combustion occur (that is, when the progress variable increases). This fuel is therefore integrally transferred in the burned gases region $F^b$. The source term $\bar{\dot{\omega}}^{u\to b}_{Fu}$ accounts for these fuel mass transfers, and it appears therefore with opposite signs in the unburned and burned fuel equations. The reaction rate $\bar{\dot{\omega}}^u_{Fu}$ represents the oxidation of unburned fuel by AI or PF. The reaction rate $\bar{\dot{\omega}}^b_{Fu}$ represents the oxidation of burned fuel by a DF.

The ECFM3Z model allows a multi-fuel description based on the method presented for the ECFM model in Colin *et al.* (2003). In this case, the fuel species $\tilde{Y}^u_{Fu}$ and $\tilde{Y}^b_{Fu}$ are replaced by their components $\tilde{Y}^u_{Fu_i}$ and $\tilde{Y}^b_{Fu_i}$ with *i* ranging from 1 to N, N being the total number of fuel components. For the sake of simplicity, only the single component case is presented here.

## 2.2 Definition of the Progress Variable $\tilde{c}$ and Tracers

The CFM model is based on the assumption that the flame can be seen as an infinitely thin interface separating fresh and burned gases. Each species in the unburned gases is consumed by AI or PF proportionally to its mass fraction in these gases. Therefore, the conservation of mass through the flame front allows the local burned mass fraction $\tilde{c}$ to be proportional to the fraction of fuel mass that has been oxidized since the beginning of combustion:

$$\tilde{c}=1-\frac{\overline{m}^u}{\overline{m}}=1-\frac{\tilde{Y}^u_{Fu}}{\tilde{Y}_{TFu}} \quad (6)$$

where $\tilde{Y}_{TFu}$ is the mass fraction of fuel before the onset of combustion. $\tilde{Y}_{TFu}$ is constant in space and time for perfectly mixed charges. In this case, the calculation of $\tilde{c}$ is straightforward. In practical applications, $\tilde{Y}_{TFu}$ varies in space and time due to the imperfect mixing of the charge. In order to calculate $\tilde{Y}_{TFu}$ exactly, we introduce an equation for the fuel tracer $\bar{\rho}_{TFu}=\bar{\rho}\tilde{Y}_{TFu}$. By definition, the tracer of a species *x* is convected and diffused exactly like the real species it represents, but unlike the species *x*, this pseudo-species is not consumed during combustion nor accounted for in thermodynamic balances. Therefore its evolution equation is the same as the one for *x* without the reaction term:

$$\frac{\partial \bar{\rho}\tilde{Y}_{Tx}}{\partial t}+\frac{\partial \bar{\rho}\tilde{u}_i\tilde{Y}_{Tx}}{\partial x_i}=\frac{\partial}{\partial x_i}\left(\left(\frac{\mu}{Sc}+\frac{\mu_t}{Sc_t}\right)\frac{\partial \tilde{Y}_{Tx}}{\partial x_i}\right)+\bar{\rho}\tilde{\dot{S}}_x \quad (7)$$

$\tilde{Y}_{TFu}$ is alternatively defined as the mean mixture fraction in other combustion models.

It can be seen from Equation (6) that the progress variable $\tilde{c}$ is only defined if $\tilde{Y}_{TFu} > 0$. If this condition is not satisfied, it indicates that the cell never contained fuel, in which case combustion could not occur. Therefore in practice, the combustion model is not applied to a cell if $\tilde{Y}_{TFu} - Y^F_{Fu}$ is inferior to a prescribed small value.

Finally, tracer equations are also solved for $O_2$, CO, NO, $H_2$ and soot. These quantities will be used to compute the fresh gases state composition. They also allow to transfer minor species CO, NO, $H_2$ and soot from burned to fresh gases in the case of multiple injection as explained in Section 2.5.

## 2.3 Computation of Mixed and Unmixed Species

### 2.3.1 The Mixing Model

In order to describe the three mixing zones presented in the principle of the model, we introduce two new quantities: the unmixed fuel (with mass fraction $\tilde{Y}^F_{Fu}$) which represents the fuel contained in regions $F^u$ and $F^b$ in Figure 1, and the unmixed oxygen (with mass fraction $\tilde{Y}^A_{O_2}$) which represents the oxygen contained in regions $A^u$ and $A^b$. $\bar{\rho}\tilde{Y}^F_{Fu}$ (resp. $\bar{\rho}\tilde{Y}^A_{O_2}$) represents a fraction of the total mass of the fuel $\bar{\rho}\tilde{Y}^u_{Fu} + \bar{\rho}\tilde{Y}^b_{Fu}$ (resp. the total mass of the oxygen $\bar{\rho}\tilde{Y}_{O_2}$). Therefore, these species do not enter in the global species mass balance and are therefore qualified "fictitious species". The equations for these unmixed species are:

$$\frac{\partial \bar{\rho}\tilde{Y}^F_{Fu}}{\partial t} + \frac{\partial \bar{\rho}\tilde{u}_i\tilde{Y}^F_{Fu}}{\partial x_i} = \frac{\partial}{\partial x_i}\left(\left(\frac{\mu}{Sc} + \frac{\mu_t}{Sc_t}\right)\frac{\partial \tilde{Y}^F_{Fu}}{\partial x_i}\right) + \bar{\rho}\tilde{\dot{S}}_{Fu} + \bar{\rho}\tilde{\dot{E}}^{F\to M}_{Fu} \tag{8}$$

$$\frac{\partial \bar{\rho}\tilde{Y}^A_{O_2}}{\partial t} + \frac{\partial \bar{\rho}\tilde{u}_i\tilde{Y}^A_{O_2}}{\partial x_i} = \frac{\partial}{\partial x_i}\left(\left(\frac{\mu}{Sc} + \frac{\mu_t}{Sc_t}\right)\frac{\partial \tilde{Y}^A_{O_2}}{\partial x_i}\right) + \bar{\rho}\tilde{\dot{E}}^{A\to M}_{O_2} \tag{9}$$

The evaporation source term $\bar{\rho}\tilde{\dot{S}}_{Fu}$ in the unmixed fuel equation is the gaseous fuel mass production rate already presented for the unburned and burned fuel equations.

The mixing model itself is described by the source terms $\tilde{\dot{E}}^{F\to M}_{Fu}$ and $\tilde{\dot{E}}^{A\to M}_{O_2}$. We consider the mixing rate of the fuel to be proportional to its volume fraction $\tilde{X}^F_{Fu}$ and a mixing time-scale $\tau_m$:

$$\tilde{\dot{E}}^{F\to M}_{Fu} = -\frac{1}{\tau_m}\tilde{X}^F_{Fu}(1-\tilde{X}^F_{Fu}) \tag{10}$$

By writing the volume fraction as a function of the mass fraction, we find:

$$\tilde{\dot{E}}^{F\to M}_{Fu} = -\frac{1}{\tau_m}\tilde{Y}^F_{Fu}\left(1-\tilde{Y}^F_{Fu}\frac{\bar{\rho}M^M}{\bar{\rho}^u|_u\, M_{Fu}}\right) \tag{11}$$

Following the same reasoning, we obtain the following expression for the mixing rate of the oxygen:

$$\tilde{\dot{E}}^{A\to M}_{O_2} = -\frac{1}{\tau_m}\tilde{Y}^A_{O_2}\left(1-\frac{\tilde{Y}^A_{O_2}}{\tilde{Y}^\infty_{O_2}}\frac{\bar{\rho}M^M}{\bar{\rho}^u|_u\, M_{air+EGR}}\right) \tag{12}$$

Where $M^M$ is the mean molar mass of the gases in the mixed area, $M_{Fu}$ is the molar mass of fuel, $M_{O_2}$ is the molar mass of $O_2$, $M_{air+EGR}$ is the mean molar mass of unmixed air + EGR gases, $\bar{\rho}$ is mean density, $\bar{\rho}^u|_u$ is the density of the unburned gases, $\tilde{Y}^\infty_{O_2}$ is the oxygen mass fraction in the unmixed air.

The mixing time-scale $\tau_m$ is considered proportional to the turbulent time-scale given by the $k$-ε model:

$$\tau_m^{-1} = \beta_m\frac{\varepsilon}{k} \tag{13}$$

where $\beta_m$ is a constant set to 1.

The oxygen concentration in the unmixed air is computed as follows:

$$\tilde{Y}^\infty_{O_2} = \frac{\tilde{Y}_{TO_2}}{1-\tilde{Y}_{TFu}} \tag{14}$$

where subscripts $TO_2$ and $TFu$ represent oxygen and fuel tracers respectively.

For the other species $X$ transported, we assume that the unburned gas composition of air + EGR is the same in the mixed and unmixed areas. Thus, if we know the total amount of oxygen (the oxygen tracer) and unmixed oxygen, we know the mass ratio $c^A_{O_2}$ of unmixed air + EGR over total air + EGR:

$$c^A_{O_2} = \frac{\tilde{Y}^A_{O_2}}{\tilde{Y}_{TO_2}} = \frac{\tilde{Y}^A_X}{\tilde{Y}_{TX}} \tag{15}$$

Where $\tilde{Y}_{TX}$ is the concentration of the tracer of species $X$ and $\tilde{Y}^A_X$ is the concentration of its unmixed part. For species $O_2$, CO, NO, soot and $H_2$, we have specified previously that a transport equation is directly solved for their tracers. For species $N_2$, $CO_2$ and $H_2O$, the tracers are reconstructed from the N, C and H atom balance equations:

$$\tilde{Y}_{TN_2} = \frac{\bar{\rho}_{N_2} + \bar{\rho}_N + \frac{M_N}{M_{NO}}(\bar{\rho}_{NO} - \bar{\rho}_{TNO})}{\bar{\rho}} \tag{16}$$

$$\tilde{Y}_{TCO_2} = \left(\frac{\bar{\rho}^u_{Fu} + \bar{\rho}^b_{Fu} - \bar{\rho}_{TFu}}{M_F}x + \frac{\bar{\rho}_{CO_2}}{M_{CO_2}} + \frac{\bar{\rho}_{CO} - \bar{\rho}_{TCO}}{M_{CO}}\right)\frac{M_{CO_2}}{\bar{\rho}} \tag{17}$$

$$\tilde{Y}_{TH_2O} = \left(\frac{\bar{\rho}^u_{Fu} + \bar{\rho}^b_{Fu} - \bar{\rho}_{TFu}}{M_{Fu}}y + 2\frac{\bar{\rho}_{H_2O}}{M_{H_2O}} + 2\frac{\bar{\rho}_{H_2} - \bar{\rho}_{TH_2}}{M_{H_2}} + \frac{\bar{\rho}_{OH}}{M_{OH}} + \frac{\bar{\rho}_H}{M_H}\right)\frac{M_{H_2O}}{2\bar{\rho}} \tag{18}$$

where $x$ and $y$ are the number of carbon and hydrogen atoms respectively per molecule of mean fuel. $M_X$ (resp. $M_{TX}$) is the molar mass of species $X$ (resp. tracer of species $X$).

Thus for a given cell, the fraction of mass which is not in the mixed area is:

$$\tilde{Y}^{A+F} = \frac{\overline{\rho}^{A+F}}{\overline{\rho}} = c^A_{O_2}(\tilde{Y}_{TO_2} + \tilde{Y}_{TH_2} + \tilde{Y}_{TCO_2} + \tilde{Y}_{TCO} + \tilde{Y}_{TH_2O} + \tilde{Y}_{TN_2} + \tilde{Y}_{TNO}) + \tilde{Y}^F_{Fu} \quad (19)$$

If $\tilde{Y}^{A+F} < 0.95$ we compute the properties of the mixed area. Otherwise, we consider that mixing is not advanced enough for combustion to take place.

### 2.3.2 Conditional Compositions in the Mixed Zone

Global and unmixed species were previously introduced. Knowing these quantities, we are now able to define the mixed quantities by simply applying the mass conservation of species in the cell:

$$\overline{\rho}^M_X = \overline{\rho}\tilde{Y}^M_X = \overline{\rho}_X - \overline{\rho}^A_X = \overline{\rho}\tilde{Y}_X - \overline{\rho}_X\tilde{Y}^A_X \quad (20)$$

Mass densities of species tracers in the mixed area are also obtained directly from the difference between species tracers and unmixed quantities:

$$\overline{\rho}^M_{TX} = \overline{\rho}\tilde{Y}^M_{TX} = \overline{\rho}_{TX} - \overline{\rho}^A_X = \overline{\rho}\tilde{Y}_{TX} - \overline{\rho}\tilde{Y}^A_X \quad (21)$$

For the unburned and burned fuel densities, we have to subtract the unmixed fuel contained in the unburned and burned zones:

$$\begin{aligned}\overline{\rho}^{u,M}_{Fu} &= \overline{\rho}\tilde{Y}^{u,M}_{Fu} = \overline{\rho}^u_{Fu} - \overline{\rho}^{u,F}_{Fu} = \overline{\rho}\tilde{Y}^u_{Fu} - \overline{\rho}\tilde{Y}^{u,F}_{Fu}\\ \overline{\rho}^{b,M}_{Fu} &= \overline{\rho}\tilde{Y}^{b,M}_{Fu} = \overline{\rho}^b_{Fu} - \overline{\rho}^{b,F}_{Fu} = \overline{\rho}\tilde{Y}^b_{Fu} - \overline{\rho}\tilde{Y}^{b,F}_{Fu}\end{aligned} \quad (22)$$

where the unmixed unburned (resp. burned) fuel mass fractions are defined by:

$$\begin{aligned}\overline{\rho}^{u,F}_{Fu} &= \overline{\rho}\tilde{Y}^{u,F}_{Fu} = (1-\tilde{c})\overline{\rho}^F_{Fu}\\ \overline{\rho}^{b,F}_{Fu} &= \overline{\rho}\tilde{Y}^{b,F}_{Fu} = \tilde{c}\overline{\rho}^F_{Fu}\end{aligned} \quad (23)$$

In order to apply the combustion model in the mixed zone, we need to define the conditioned densities $\overline{\rho}^M_X|_M$ in the mixed area which are related to unconditioned densities $\overline{\rho}^M_X$ through the relation:

$$\overline{\rho}^M_X|_M = \frac{\overline{m}^M_X}{V^M} = \frac{\overline{m}^M_X}{V}\frac{V}{V^M} = \overline{\rho}^M_X C_{VM} = \overline{\rho}^M|_M\ \tilde{Y}^M_X|_M \quad (24)$$

The volume fraction $C_{VM}$ is deduced from the volume conservation in the cell ($V = V^M + V^{A+F}$, where $V^X$ is the volume of zone $X$):

$$C_{VM} = \frac{\overline{\rho}^u|_u}{\overline{\rho}^u|_u - \overline{\rho}^{A+F}} = \frac{V}{V^M} \quad (25)$$

where $\overline{\rho}^u|_u$ is the mass density of unburned gases conditioned in these gases, and is deduced from the mean pressure $p$ and the fresh gases temperature $T^u$. The mean density conditioned in the mixed area $\overline{\rho}^M|_M$ is simply given by:

$$\overline{\rho}^M|_M = (\overline{\rho} - \overline{\rho}^{A+F})C_{VM} \quad (26)$$

Knowing $C_VM$ and $\overline{\rho}^M|_M$, we can now compute the conditioned mass densities for species $\overline{\rho}^M_X|_M$, species tracers $\overline{\rho}^M_{TX}|_M$, unburned and burned fuel $\overline{\rho}^{u,M}_{Fu}|_M$ and $\overline{\rho}^{b,M}_{Fu}|_M$ using relation (24).

As for species, we need to define the mean conditioned enthalpy in the mixed area:

$$\tilde{h}^M = \tilde{h} + (\tilde{h} - \tilde{h}^u)\frac{\overline{\rho}^{A+F}}{\overline{\rho} - \overline{\rho}^{A+F}} \quad (27)$$

where $\tilde{h}^u$ is the fresh gases enthalpy defined by its evolution equation (Colin *et al.*, 2003).

All the operations previously done in the ECFM model over global quantities are now done on the conditional concentrations in the mixed zone. Often, the species molar concentrations are used in the combustion model, instead of the species densities, the two being related by:

$$\overline{N}^M_X|_M = \frac{\overline{\rho}^M_X|_M}{M_X} \quad (28)$$

In the following parts, we briefly explain how the combustion model is applied to the mixed area.

Once the reaction rates describing AI, PF and DF have been computed, the species densities $\overline{\rho}^M_X|_M$ and the enthalpy $\tilde{h}^M$ are updated. In order to recover the updated global densities and enthalpy, the previous operations are performed in the reverse sense.

## 2.4 Conditional Compositions in Fresh and Burned Gases of the Mixed Zone

We have shown how we could define, starting from the mean species concentrations and enthalpies, the equivalent quantities in the mixed zone. The ECFM model can now be applied to the mixed zone. In this model, the flame front is described as an infinitely thin interface that separates fresh and burned gases. In order to correctly compute the laminar flame speed in the fresh gases and the pollutant kinetics in the burned gases we need to precisely define the properties in these regions. The mass fractions $\tilde{Y}^{u,M}_x|_{u,M}$ and $\tilde{Y}^{b,M}_x|_{b,M}$ in these regions are defined as:

$$\tilde{Y}^{u,M}_x|_{u,M} = \frac{\overline{m}^{u,M}_x}{\overline{m}^{u,M}} \quad (29)$$

$$\tilde{Y}^{b,M}_x|_{b,M} = \frac{\overline{m}^{b,M}_x}{\overline{m}^{b,M}} \quad (30)$$

where $\overline{m}^{u,M}$ (resp. $\overline{m}^{b,M}$) is the unburned (resp. burned) mass in the mixed zone defined by:

$$\begin{aligned}\overline{m}^{u,M} &= (1-\tilde{c})\overline{m}^{M} \\ \overline{m}^{b,M} &= \tilde{c}\overline{m}^{M}\end{aligned} \tag{31}$$

where $\overline{m}^{M}$ is the total mass in the mixed zone of the cell. It is defined by: $\overline{m}^{M} = (\overline{\rho} - \overline{\rho}^{A+F})V = \overline{\rho}^{M}|_{M} V_{M}$.

Using a mass balance equation $\tilde{Y}_{x}^{M}|_{M}$ can be written:

$$\begin{aligned}\tilde{Y}_{x}^{M}|_{M} &= \frac{\overline{m}_{x}^{M}}{\overline{m}^{M}} = \frac{\overline{m}_{x}^{u,M} + \overline{m}_{x}^{b,M}}{\overline{m}^{M}} \\ \tilde{Y}_{x}^{M}|_{M} &= \tilde{Y}_{x}^{u,M}|_{M} + \tilde{Y}_{x}^{b,M}|_{M}\end{aligned} \tag{32}$$

Then by combing with Equations (29), (30) and (31) we obtain:

$$\tilde{Y}_{x}^{M}\big|_{M} = (1-\tilde{c})\tilde{Y}_{x}^{u,M}\big|_{u,M} + \tilde{c}\tilde{Y}_{x}^{b,M}\big|_{b,M} \tag{33}$$

where $\tilde{c}$ is the local burned mass fraction previously defined. We remark that quantities $\tilde{Y}_{x}^{u,M}\big|_{M}$ and $\tilde{Y}_{x}^{u,M}\big|_{u,M}$ are conditioned over different zones:

- $\tilde{Y}_{x}^{u,M}\big|_{M}$ compares the mass of the species *x*, contained in the fresh gases of the mixed zone, to the total mixed mass $\overline{m}^{M}$ *(see Eq. (32))*;
- $\tilde{Y}_{x}^{u,M}\big|_{u,M}$ is the "real" average mass fraction of species *x* in the fresh gases of the mixed zone *(see Eq. (29))*.

In other words, $\tilde{Y}_{x}^{u,M}\big|_{M}$ represents the mass fraction of the mixed unburned part of species *X* conditioned on only one zone (the mixed zone) and $\tilde{Y}_{x}^{u,M}\big|_{u,M}$ represents the same part of the species but conditioned on two zones simultaneously (the mixed and the unburned zones).

Of course, the same difference between $\tilde{Y}_{x}^{b,M}\big|_{M}$ and $\tilde{Y}_{x}^{b,M}\big|_{b,M}$, can be noticed.

### 2.4.1 Fresh Gases State

In the ECFM model (Colin *et al.*, 2003), we have assumed that fresh gases were composed of fuel, $O_2$, $N_2$, $CO_2$ and $H_2O$. We now add species $H_2$, CO, NO and soot to this composition in order to have a better description of the real composition of the fresh gases. However each new species in the fresh gases imposes the addition of a species tracer, otherwise the fresh gases composition cannot be determined.

The fuel mass fraction in the fresh gases $\tilde{Y}_{F}^{u,M}\big|_{u,M}$ is simply given by:

$$\tilde{Y}_{Fu}^{u,M}|_{u,M} = \frac{\overline{\rho}_{TFu}^{M}}{\overline{\rho}^{M}} = \tilde{Y}_{TFu}^{M}|_{M} \tag{34}$$

This equality states that the fresh gases mixture composition is the same as the average composition we would get if no combustion had occurred. This average composition is exactly the one given by the fuel tracer in the mixed region. Using the definitions of the mixed tracers $\tilde{Y}_{TX}^{M}\big|_{M}$ for the other species, we can apply the same argument for the mass fraction $\tilde{Y}_{X}^{u,M}\big|_{u,M}$:

$$\tilde{Y}_{X}^{u,M}|_{u,M} = \frac{\overline{\rho}_{TX}^{M}}{\overline{\rho}^{M}} = \tilde{Y}_{TX}^{M}|_{M} \tag{35}$$

The fresh gases temperature $\tilde{T}^{u}$ is obtained by inversion of the fresh gases enthalpy $\tilde{h}^{u}$ based on the fresh gases mass fractions $\tilde{Y}_{X}^{u,M}\big|_{u,M}$.

### 2.4.2 Burned Gases State

The burned gases composition and temperature $\tilde{T}^{b}$ are used in the model to compute some flame characteristics as well as pollutant production and post-oxidation (for DF combustion). This composition includes species O, OH, H and N issued from equilibrium calculations. The fuel mass fraction in the burned gases is obtained by conditioning the burned fuel $\overline{m}_{Fu}^{b}$ in the mixed zone and then in the burned gases zone as described previously. The other species in the burned gases are rebuilt from the average and fresh gases states using Equation (33):

$$\tilde{Y}_{x}^{b,M}|_{b,M} = \frac{\tilde{Y}_{x}^{M}|_{M} - (1-\tilde{c})\tilde{Y}_{x}^{u,M}|_{u,M}}{\tilde{c}} \tag{36}$$

We note that the mass fraction of species O, OH, H, and N in the fresh gases is zero.

In ECFM3Z the unmixed areas *F* and *A* are supposed to be at the unburned gases temperature $\tilde{T}^{u}$ of the mixed unburned zone $M^{u}$, while only gases of zone $M^{b}$ are at temperature $\tilde{T}^{b}$. We need therefore to know the exact mass fraction occupied by this zone. We first define a coefficient $C_{m^M} = \frac{\overline{m}^{u,M} + \overline{m}^{b,M}}{\overline{m}}$ that takes into account the fraction of mixed mass, which is simply the total mass minus the mass of the pure fuel zone minus the mass of the pure air zone. This can be deduced from Equation (19):

$$C_{m^M} = 1 - \tilde{Y}^{A+F} = 1 - \tilde{Y}_{Fu}^{F} - (1-\tilde{Y}_{TFu})\frac{\tilde{Y}_{O_2}^{A}}{\tilde{Y}_{TO_2}} \tag{37}$$

We can now define the mass fraction of zone $M^{b}$:

$$\tilde{c}_{b,M} = \frac{\overline{m}^{b,M}}{\overline{m}} = \frac{\overline{m}^{b,M}}{\overline{m}^{M}}\frac{\overline{m}^{M}}{\overline{m}} = \tilde{c}C_{m^M} \tag{38}$$

The fraction $1-\tilde{c}_{b,M}$ is then exactly the mass fraction at the fresh gases temperature $T^{u}$, corresponding to zones $F^{u}$, $F^{b}$, $A^{u}$, $A^{b}$ and $M^{u}$ in Figure 1.

The burned gases enthalpy $\tilde{h}^{b}$ can now be deduced from the energy balance equation:

$$\tilde{h} = (1-\tilde{c}_{b,M})\tilde{h}^{u} + \tilde{c}_{b,M}\tilde{h}^{b} \tag{39}$$

If $\tilde{c}_{b,M}$ is too small, the above relation can not be used, and a more simple estimate of $\tilde{h}^{b}$ is used instead (Colin *et al.*, 2003).

### 2.5 Treatment of Multiple Injections

When the fuel contained in fresh gases, corresponding to $\widetilde{Y}^{u}_{Fu}$, has been completely burned, the progress variable $\widetilde{c}$ equals one. In this case, the mixed region is only composed of burned gases. If after this instant, gaseous fuel is added through evaporation of fuel droplets (term $\dot{\overline{S}}_{Fu}$ in *Eq. (5), (7)* and *(8)*), the fuel tracer mass fraction $\widetilde{Y}_{TFu}$ and the fuel contain in burned gases $\widetilde{Y}^{b}_{Fu}$ increase, but the progress variable remains equal to one because $\widetilde{Y}^{u}_{Fu}$ remains equal to zero. This situation is found when burned gases temperature is high enough to oxidise rapidly the fuel coming from the unmixed fuel region. As explained previously, this situation represents in a simple way combustion by a diffusion flame. On the contrary, if burned gases temperature is low, chemical reactions in burned gases stop and fuel contained in burned gases of the mixed region will not be oxidised anymore. At this point it would be necessary to consider combustion by auto-ignition which would eventually reignite the mixture. This would imply the definition of a second progress variable in burned gases with a second fuel tracer equation. In the case of many fuel injections, a new fuel tracer would be required for each injection.

As this solution clearly complicates the model excessively, we adopted a more simple procedure. It consists in reinitialising the progress variable when combustion stops in burned gases by imposing:

$$\begin{aligned} \overline{\rho}^{u,new}_{Fu} &= \overline{\rho}^{u}_{Fu} + \overline{\rho}^{b}_{Fu} \\ \overline{\rho}^{b,new}_{Fu} &= 0 \\ \overline{\rho}^{new}_{TFu} &= \overline{\rho}^{u}_{Fu} + \overline{\rho}^{b}_{Fu} \end{aligned} \qquad (40)$$

Conditions given by Equation (40) are progressively imposed in time and they allow to transfer fuel from burned to fresh gases and to progressively make the progress variable tend towards zero. This procedure does not change species composition since fuel is transferred from one equation to the other and fuel tracer is a fictive species which does not enter the mass balance. When the progress variable has been reinitialised, a new computation of combustion by auto-ignition can start.

Finally, this procedure allows to treat multiple injection cases very often found in recent Diesel engines.

## 3 FUEL OXIDATION MODELS

As specified in Section 1, the three main modes of combustion, namely auto-ignition (AI), premixed propagation flame (PF) and diffusion flame (DF) are represented in the ECFM3Z model. These three modes can occur simultaneously in the mixed zone *M*. The AI and PF models predict an instantaneous reaction rate $\dot{\overline{\omega}}^{u}_{Fu}$ applied to the unburned fuel, *Eq. (4)*. These models are not detailed here as they can be found in (Colin *et al.*, 2003) and (Colin *et al.*, 2004), so we suppose here that the fuel reaction rate is given and we focus instead on the fuel decomposition into products that enter the burned gases region $M^b$.

For the DF, the mixing model presented previously allows to transfer the unmixed fuel of region $F^b$ in the burned gases of region $M^b$. We present here the model used in region $M^b$ for the burned fuel reaction rate $\dot{\overline{\omega}}^{b}_{Fu}$ appearing in Equation (4). Finally, we present the post-flame kinetics in this region that allow to complete the fuel oxidation (transformation of CO in $CO_2$) and to predict pollutant formation as well as chemical equilibrium.

### 3.1 Unburned Fuel Oxidation

In order to account for the partial oxidation of fuel into CO and $CO_2$, the fuel oxidation is decomposed into two phases:

– A first partial oxidation of fuel is performed which leads to the formation of a major fraction of CO and some $CO_2$ in the burned gases of the mixed zone.
– In the burned gases of the mixed zone, the CO previously generated is oxidised into $CO_2$. This second phase will be presented in Section 3.3.

The oxidation of the unburned fuel into CO, $CO_2$, $H_2$ and $H_2O$ is performed by the three following reactions:

$$\begin{aligned} &\alpha(1-r_{CO})[C_xH_y + (x+\frac{y}{4})O_2 \rightarrow xCO_2 + \frac{y}{2}H_2O] \\ &\alpha r_{CO}[C_xH_y + (\frac{x}{2}+\frac{y}{4})O_2 \rightarrow xCO + \frac{y}{2}H_2O] \\ &(1-\alpha)[C_xH_y + \frac{x}{2}O_2 \rightarrow xCO + \frac{y}{2}H_2] \end{aligned} \qquad (41)$$

The coefficient $\alpha$ is defined by the local equivalence ratio:

$$\begin{aligned} &\text{if } \overline{\phi} < 1 && \rightarrow \alpha = 1 \\ &\text{if } 1 \le \overline{\phi} < \phi_{crit} && \rightarrow \alpha = \frac{\frac{4(x+\frac{y}{4})}{\overline{\phi}} - 2x}{2x+y} \\ &\text{if } \phi_{crit} \le \overline{\phi} && \rightarrow \alpha = 0 \end{aligned} \qquad (42)$$

where the critical equivalence ratio $\phi_{crit}$ is defined by $\phi_{crit} = \frac{2}{x}(x+\frac{y}{4})$.

For lean mixtures $\alpha = 1$, which means only the first two reactions in (41) are considered. In a previous version of the model, we considered $r_{CO} = 0$, which means the fuel was completely oxidised into $CO_2$ and $H_2O$ through the first reaction of (41). As experiments and complex chemistry calculations showed that CO could be formed even in lean mixtures provided the equivalence ratio is very low (below 0.3 according to Dec (2002)), we introduced the second

reaction in (41) which allows the formation of CO even for lean mixtures. The proportion of CO and $CO_2$ formed is monitored by the coefficient $r_{CO}$ which is assumed, as a first model, to be a constant equal to 0.9. In the future, this coefficient could be given by complex chemistry calculations for different values of temperature, equivalence ratio, EGR rate.

If $\overline{\phi}$ is larger than unity, the oxygen mass fraction in the fresh gases is not sufficient to completely oxidise the fuel into $CO_2$ and $H_2O$. The third reaction, which transforms fuel into CO and $H_2$ becomes predominant. If $\overline{\phi}$ becomes larger than the critical value $\phi_{crit}$, the amount of oxygen in the fresh gases does not even allow to perform the partial oxidation of fuel into CO. In this case, a part of the unburned fuel is transferred as burned fuel in zone $M^b$. This corresponds to the source term $\overline{\dot{\omega}}_{Fu}^{u\to b}$ in Equation (4) but conditioned in the mixed zone $M$:

$$\overline{\dot{\omega}}_{Fu}^{u\to b}\,|_M = -\overline{\dot{\omega}}_{Fu}^{u,M}\,|_M\,\left(1-\frac{\phi_{crit}}{\overline{\phi}}\right) \tag{43}$$

### 3.2 Fuel Post-Oxidation in Burned Gases

The description adopted for gases state considers all species contained in region $M^b$ to be perfectly mixed. Consequently the DF model, used to post-oxidise the fuel of this region (*i.e.* the fuel resulting from transfer mechanisms, described in the previous sections, into $M^b$), should be entirely controlled by the chemistry. It is the reason why we adopt a model based on a chemical time scale $\tau_c$:

$$\overline{\dot{\omega}}_{Fu}^{b,M}\,|_{b,M} = -\frac{\overline{\rho}\,\tilde{Y}_{Fu}^{b,M}\,|_{b,M}}{\tau_c} \tag{44}$$

where:

$$\tau_c = A e^{\frac{Ta}{\tilde{T}^b}} \tag{45}$$

with $A = 2\times10^{-6}$ and $Ta = 6000$ K. The constant $A$ and the activation temperature $Ta$ have been chosen by comparing computation and experiment on an engine case. The reaction rate $\overline{\dot{\omega}}_{Fu}^{b,M}\big|_{b,M}$ of the fuel contained in burned gases is then used to deduce reaction rates of the other species following a procedure similar to that adopted in fresh gases (*Eq. (41)*). The only difference is that we assume $r_{CO} = 1$ in $M^b$.

### 3.3 Post-Flame Kinetics

Post-flame chemical equilibrium and pollutant formation are computed to correct the burned gases state and temperature. The post-flame chemistry of the model is an improved version of the post-flame chemistry of the ECFM model (Colin, 2003). The major changes are the addition of a soot model (Martinot *et al.*, 2001) and the introduction of a kinetic oxidation of CO. Thus, the $CO/CO_2$ equilibrium is not considered any more in the equilibrium equations. An equilibrium resolution of the remaining set of equations has been rewritten. The considered equilibrium reactions are:

$$\begin{aligned} &N_2 \leftrightarrow 2N \\ &O_2 \leftrightarrow 2O \\ &H_2 \leftrightarrow 2H \\ &2OH \leftrightarrow O_2 + H_2 \\ &2H_2O \leftrightarrow O_2 + 2H_2 \end{aligned} \tag{46}$$

These equations can be reduced to one polynomial equation ($6^{th}$ degree). This equation is then solved using a Newton method, which is straightforward with a polynomial expression.

The kinetic oxidation of CO we have considered is:

$$CO + OH \leftrightarrow CO_2 + H \tag{47}$$

where the kinetic constants for the forward and backward reactions are taken from the *n*-heptane mechanism of Curran *et al.* (1998). In this reaction OH and H are equilibrium concentrations, that is, the rate of $CO_2$ dissociation or CO oxidation does not modify their concentrations. This system is solved for using the burned gases composition and temperature.

Finally, the post-flame kinetics (including the $CO/CO_2$ kinetics, the NOx (extended version of the Zeldovich mechanism reported by Heywood, 1988) and soot (Martinot *et al.*, 2001) models (the burned fuel oxidation and the chemical equilibrium) allow to correct the estimation of the species mass fractions $\tilde{Y}_x^{b,M}\big|_{b,M}$ and the burned gases enthalpy $\tilde{h}^b$ given by the combustion models. These new estimates of $\tilde{Y}_x^{b,M}\big|_{b,M}$ and $\tilde{h}^b$ are reported to the average mass fractions $\tilde{Y}_x$ using Equation (33) and to the average enthalpy using Equation (39).

## 4 VALIDATION CASES

A parametric study on different operation points of a 4 stroke direct injection Diesel engine using a fully 3D grid was already presented in Béard *et al.* (2003). These calculations showed the ability of models developed at *IFP* to correctly reproduce the experimental trends in terms of power and pollutant emissions.

Our aim here is to focus our attention on two comparable cases on this engine in order to study the behaviour of the ECFM3Z model on typical Diesel operation points.

### 4.1 Computational Mesh and Operating Conditions

Simulations are performed using the parallel code IFP-C3D (Bohbot *et al.*, 2003; Zolver *et al.*, 2003, 2004) developed at *IFP*. This code uses an ALE (Arbitrary Lagrangian Eulerian) method to compute two-phase reactive flows in internal

combustion engines on moving unstructured hexahedral grids following a RANS approach. Calculations are performed on a wedge mesh, representing one sixth of the entire combustion chamber. Therefore, only one of the injector six holes is represented. The engine characteristics are identical to those presented in Béard *et al.* (2003) and are summarised in Table 1. The two operation points presented are summarised in Table 2. For both cases, calculations start at intake valve closure with an initial swirl flow intensity based on 3D calculations of the intake stroke. The injection and spray models are detailed in Béard *et al.* (2003). For comparison, calculations are also performed with a version of Kong's model (1995) using a reduced chemistry by Chalak (1990) for calculating the chemical time-scale. This model, which is a standard model for Diesel applications, is thereafter referred to as ECTM (extended characteristic time model). Note that for both models, the modelling constants remain unchanged for the three validation cases. The spray model used with both combustion models is also the same, which allows to assess the impact of the combustion model only.

TABLE 1

Direct injection Diesel engine characteristics

| | |
|---|---|
| Bore | 0.085 m |
| Stroke | 0.088 m |
| Connecting rod length | 0.0145m |
| Valves/cylinder | 4 |
| Intake valve opening | TDC (Top Dead Centre) |
| Intake valve closing | 146 deg. BTDC (Before TDC) |
| Exhaust valve opening | 140 deg. ATDC (After TDC) |
| Injector hole diameter | 148 $10^{-6}$ m |
| Spray angle | 152 deg. |

TABLE 2

Definition of the two operation points simulated on the direct injection Diesel engine presented in Table 1

| Case | A | B |
|---|---|---|
| Speed (rpm) | 1640 | 4000 |
| Load | partial | full |
| Start of injection (deg. BTDC) | 6. | 15.1 |
| Injection duration (deg.) | 8.03 | 37.6 |
| injected mass (g) | 0.0144 | 0.0428 |
| F/A equivalence ratio | 0.67 | 0.7 |
| EGR rate (%) | 31 | 0 |
| Initial swirl number | 2.8 | 1.4 |

## 4.2 Results and Discussion

The pressure curves and the total burned mass fractions obtained with ECFM3Z and ECTM are compared with the experimental ones in Figure 3 and Figure 4. For case B, both models predict the onset of combustion at the right instant. ECFM3Z also leads to an accurate reproduction of the onset of combustion for case A whereas ECTM predicts a too early start of combustion for the same case. This result indicates that the auto-ignition model based on tabulated chemistry in ECFM3Z (Colin *et al.*, 2004), is more reliable than the simple chemical mechanism used in ECTM.

For case A, the onset of combustion predicted by ECTM is 3.5 CA (cranck angle) degrees in advance compared to the experiment, while ECFM3Z predicts almost exactly the instant of pressure rise. Then both models predict correctly the maximum pressure but in the expansion stroke, ECTM underpredicts pressure while ECFM3Z reproduces correctly the experimental pressure. This is also seen in the final

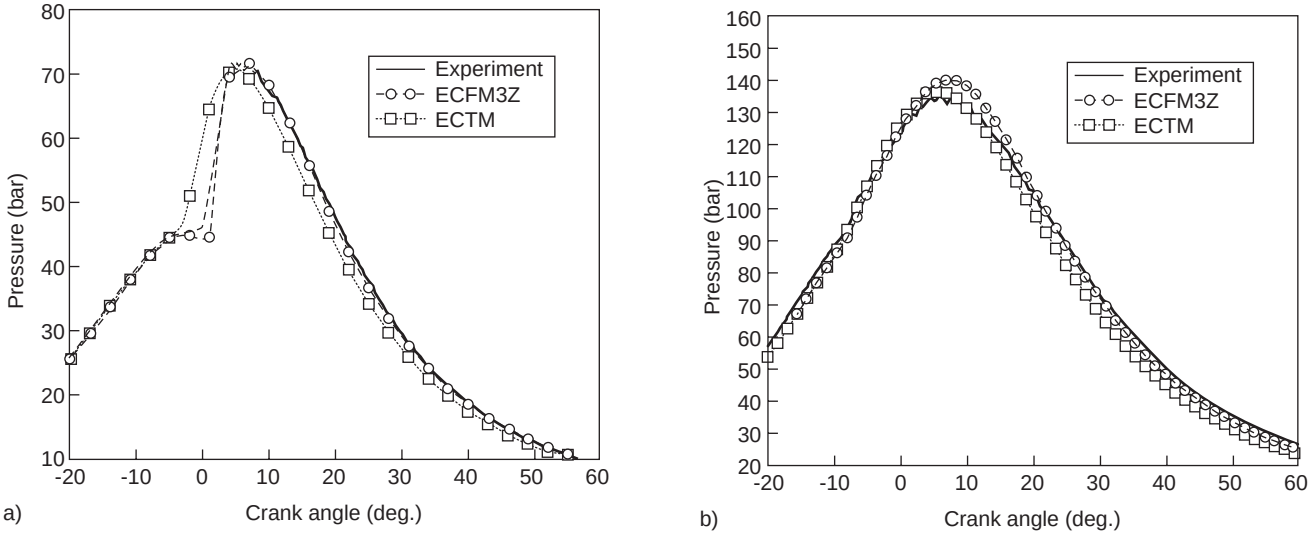


Figure 3

Pressure evolution in the chamber for cases A and B (from top to bottom).

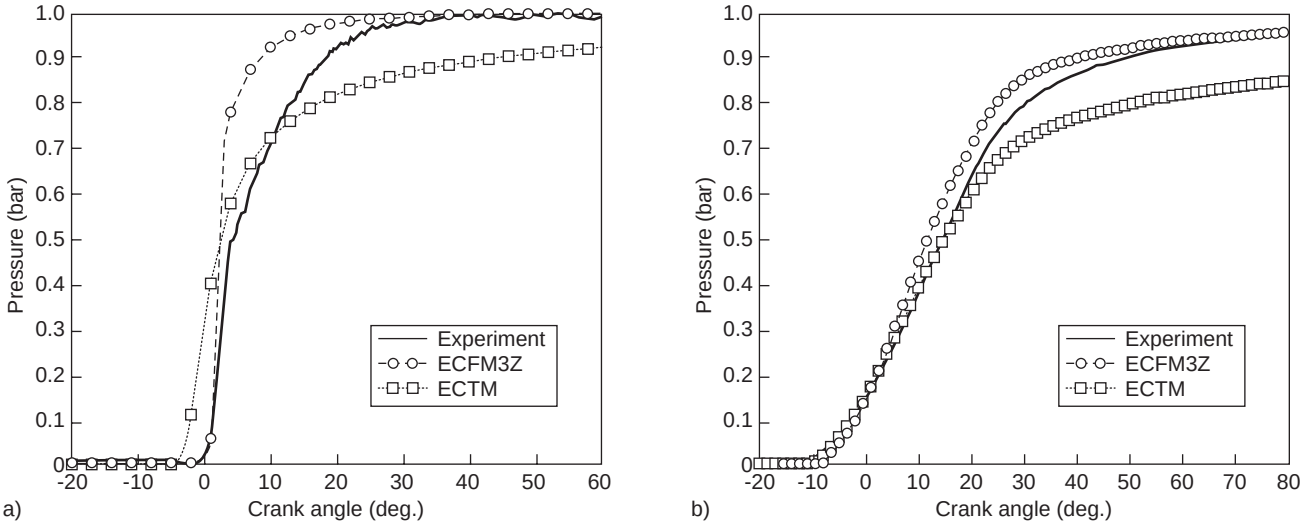


Figure 4

Temporal evolution of the total burned mass fraction for cases A and B for ECFM3Z and ECTM models.

burned mass fraction which is close to one for ECFM3Z and the experiment while ECTM reaches 0.96.

For case B, the onset of combustion is correctly predicted by both models and the maximum pressure is also correctly reproduced. The pressure evolution in the expansion stroke is underpredicted by ECTM which is correlated to the underestimated final burned mass fraction. On the contrary, pressure and burned mass fraction are correctly reproduced by ECFM3Z after top dead center.

Figure 5 presents the evolution of the total mass for the different fuel species introduced in the previous paragraphs. The fuel tracer, the unmixed fuel, the fuel in unburned gases and the fuel in burned gases correspond respectively to mass fractions $\tilde{Y}_{TFu}$, $\tilde{Y}^{F}_{Fu}$, $\tilde{Y}^{u}_{Fu}$ and $\tilde{Y}^{b}_{Fu}$. All quantities in Figure 5 are made nondimensional by dividing the mass by the total injected fuel mass. For the two cases presented here, the evaporation duration is very small compared to the injection duration, therefore, the fuel tracer mass increases roughly at the same rate as the injected fuel mass. At the end of injection, the fuel mass is equal to one, which indicates that the total injected mass has been evaporated. The injection durations are given in CA degrees for both cases in Table 2.

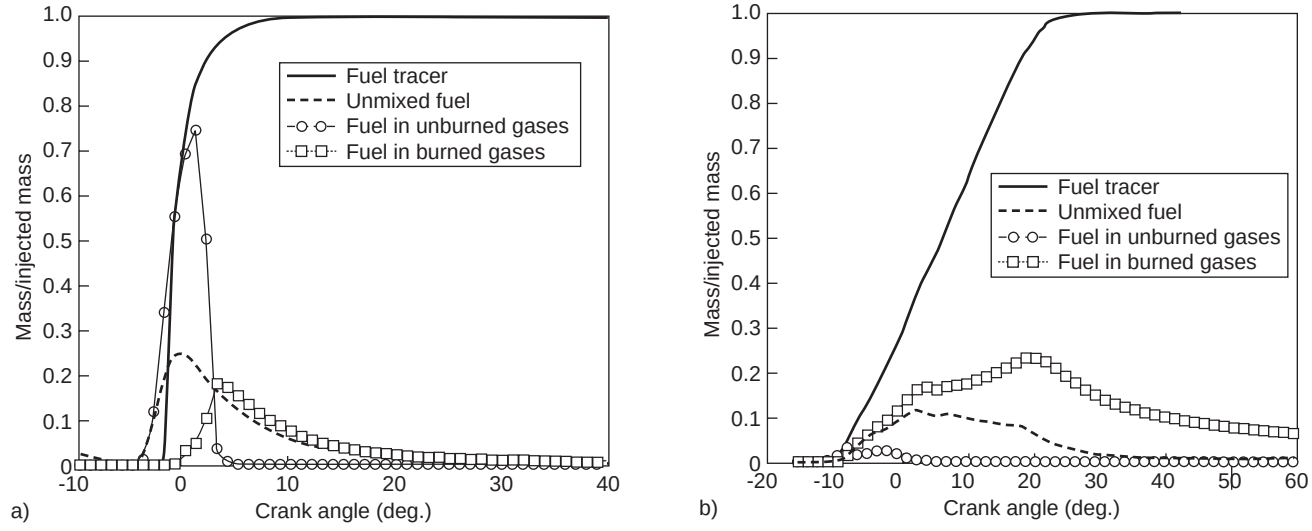


Figure 5

Temporal evolution of the different fuel species used in ECFM3Z for cases A and B (from top to bottom).

It can be seen that for case B the injection duration is much longer than for case A which is due to the higher injected mass and the higher engine speed for case B (1 CA degree represents 0.101 ms for case A and 0.0416 ms for case B).

For both cases, the fuel tracer, the unmixed fuel and the unburned fuel mass are nearly identical after the start of injection. This indicates that initially, the fuel evaporated is not mixed with air and that it is contained in the unburned gases (prior to combustion, there are no burned gases). The mixing process then tends to decrease the total unmixed fuel mass, which rapidly becomes smaller than the fuel tracer mass. Figure 6 shows for case B a 3D view of the mixed fraction defined by Equation (37) and of the mean fuel/air equivalence ratio at 2.5 CA degrees ATDC (after top dead centre). It can be seen that this fraction evolves from zero at the border of the fuel vapour cloud to one in the core of the cloud. This structure can be explained by the time history of the mixing process between fuel and air. If we consider an element of fuel mass, it is initially located at the periphery of the spray cloud, where evaporation essentially takes place, which corresponds to the core of the fuel vapor cloud. At this instant, fuel and air are perfectly unmixed, that is, the mixed fraction is close to zero. As time passes, the element of fuel mass moves away from the spray cloud and continues to mix with air, that is, its mixed fraction increases.

As auto-ignition starts in the mixed region, the unburned fuel is rapidly consumed and falls to zero. For case A, the auto-ignition delay is comparable to the evaporation time, which explains why the unburned fuel mass nearly represents the totality of the injected fuel prior to the start of auto-ignition, that is nearly all the evaporated fuel mass is contained in the unburned gases. As a consequence, the major part of the injected fuel is consumed by auto-ignition, and the creation of fuel in burned gases is very small. For case B, the auto-ignition delay is much smaller than the evaporation time. Unlike case A, the combustion by auto-ignition concerns only a very small fraction of the total fuel mass, while the essential part of the fuel evaporated is consumed by a diffusion flame.

Figure 7 presents a 3D view of the fuel contained in the unburned gases (and therefore consumed by AI) for case B: it can be seen that it is essentially located at the periphery of the vapour cloud, where the equivalence ratio is very low (that is, the fuel mass fraction is very low), while the fuel present in the burned gases is located inside the cloud, where the equivalence ratio is higher. This figure also presents the local total burned mass fraction which represents the fuel consumed by the three possible combustion modes (AI, PF and DF) defined by:

$$\tilde{c}_{tot} = 1 - \frac{\tilde{Y}_{Fu}^{u} + \tilde{Y}_{Fu}^{b}}{\tilde{Y}_{TFu}} \tag{48}$$

It can be seen that combustion is not yet started in regions containing unburned fuel, which indicates that AI in these regions has not yet begun (the auto-ignition delay has not been reached), or has just begun. On the contrary, combustion is under way in regions dominated by the diffusion flame (regions containing burned fuel).

## CONCLUSIONS

This paper has been devoted to a detailed description of a model called ECFM3Z (3-Zones Extended Coherent Flame Model). It represents a unified model that allows to compute combustion in both Diesel and gasoline engines. The main idea of ECFM3Z consists in ensuring an “accurate” description of gases state in the combustion chamber. Such a description is then used to model the three main combustion

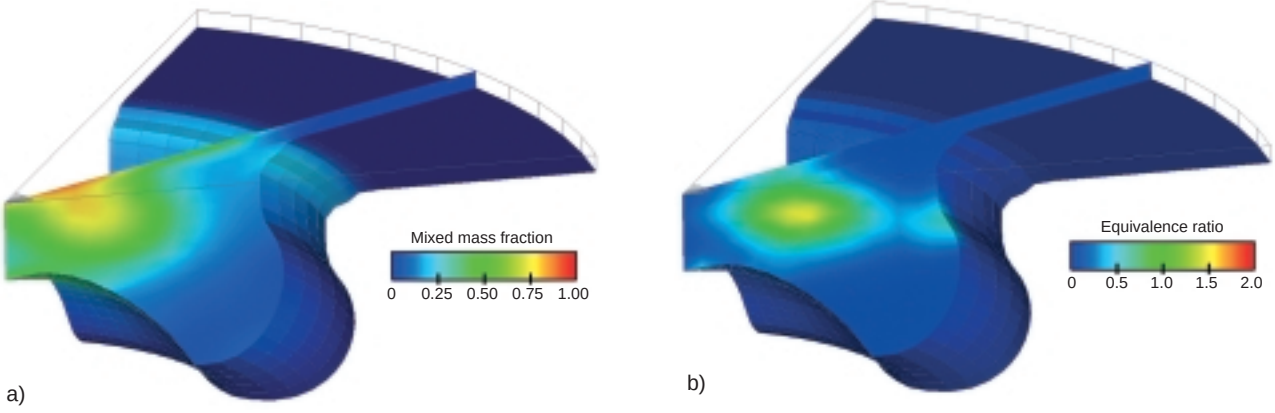


Figure 6

3D view for case B at 2.5 CA deg. After Top Dead Centre: mixed fraction (top), equivalence ratio (bottom).

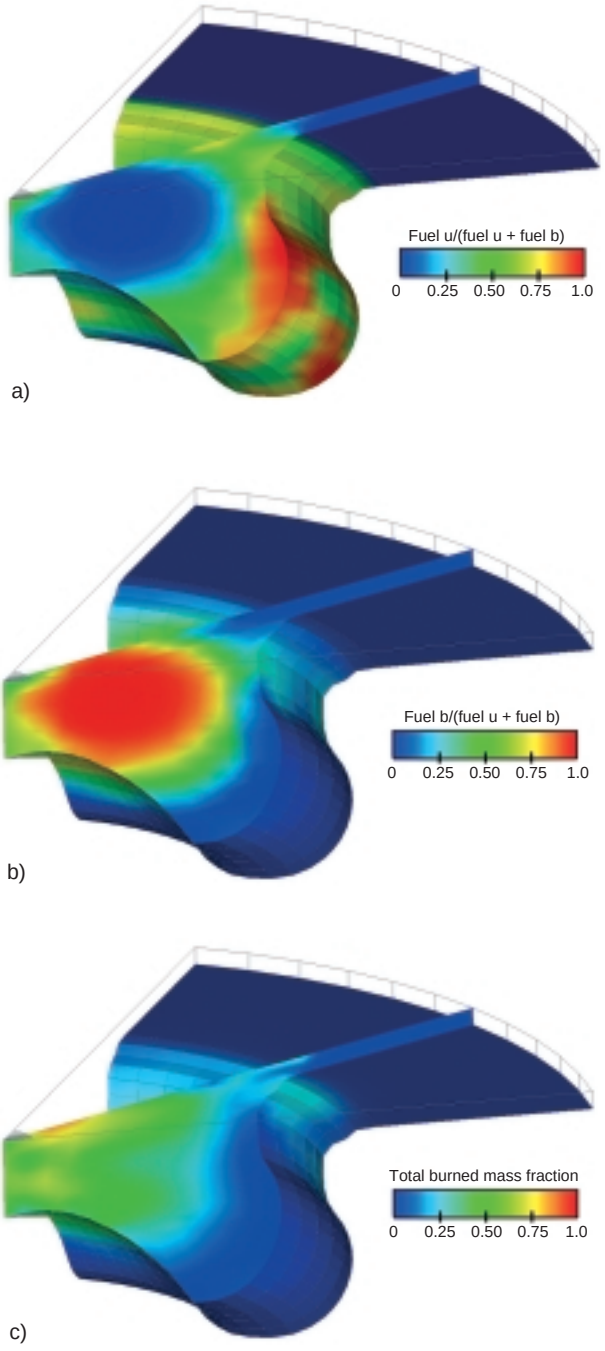


Figure 7

3D view for case B at 2.5 CA deg. After top dead centre: fraction of fuel contained in the unburned gases (top), fraction of fuel contained in the burned gases (middle), total burned mass fraction (bottom).

modes that can occur in an engine (auto-ignition, premixed flame and diffusion flame) as well as pollutant formation.

A large part of the paper has been dedicated to the 2D (Z, $\tilde{c}$) description of gases state. These gases are simultaneously described in terms of mixing (dimension Z) and combustion advancement (dimension $\tilde{c}$). The first dimension is described by a three peaks probability density function which allows to progressively create a zone where fuel and oxidiser are mixed. It is in this mixed zone that reaction rates are then computed. A precise description of the unburned gases composition and temperature including local EGR composition, is proposed. The second dimension is taken from the ECFM model (Colin *et al.*, 2003): we consider an infinitely thin reaction front that separates unburned and burned gases. The conditional averaging technique, presented in Colin *et al.* (2003), allows to properly define the gas properties in both zones. A simple model is proposed to transfer gases from the burned zone towards the unburned zone when burned gases temperature falls below a prescribed value. This way, multiple injections can be described by the model. Tracer species equations for products of reactions like NO, CO, $H_2$ and soots are added to correctly represent the formation of pollutants even in the multiple injection case.

After the description of gases state, combustion models have been discussed. For auto-ignition and premixed flame, we only referred here to recent papers describing the models developed for these combustion modes (Colin *et al.*, 2003; Colin *et al.*, 2004). However the diffusion flame description has been presented in detail. In ECFM3Z, this combustion mode is represented by two successive phases. First, a mixing model allows to transfer unmixed fuel and unmixed air in the burned gases of the mixed zone: this phase represents the turbulent diffusion of reactants towards the reaction zone. These gases then react together in the burned gases of the mixed zone, which represents the oxidation of fuel in the thin reactive layer of the diffusion flame. Finally, a brief description of post-flame kinetics is given. It is based on five equilibrium reactions and on the kinetic oxidation of fuel to CO and the oxidation of CO into $CO_2$.

Two numerical computations (cases A and B) on a direct injection Diesel engine have been performed to illustrate the behaviour of the ECFM3Z model on conventional Diesel applications. Although these two operation points differ in terms of engine speed, injected mass, injection timing and load, ECFM3Z reproduces experimental results more accurately than ECTM: the onset of combustion is always predicted at the right instant and the maximal pressure is correctly reproduced. By plotting the evolution of the different fuel species used in ECFM3Z, we observed that the dominant combustion mode differs from one case to the other, depending on the amount of fuel vapour contained in fresh gases before the onset of combustion:

– in case A (medium speed, medium load with EGR) combustion is mainly controlled by auto-ignition since most of the injected fuel has mixed with air prior to the onset of auto-ignition;
– in case B (high speed, high load) fuel injection and diffusion flame take place at the same time.

The satisfactory behaviour of ECFM3Z in both cases shows that this model correctly predicts:

- the mixing process: an accurate estimate of the mixed amount of fuel and air prior to auto-ignition is essential to correctly predict the initial pressure rise;
- the auto-ignition delay;
- the fuel post-oxidation in burned gases (especially for case B).

We did not present in this paper any validation of ECFM3Z on a gasoline engine because the premixed flame description in ECFM3Z is identical to that of the ECFM model (Colin *et al.*, 2003). This model has already been validated in previous papers, for example Duclos *et al.* (1996); Duclos and Zolver (1998); Lafossas *et al.* (2002); Colin *et al.* (2003); Henriot *et al.* (2003) and Kleemann *et al.* (2003).

Future work on this model will be devoted to the improvement of the different sub-models presented here, based on the six zones structure. The mixing model could for instance be improved by introducing a variance/scalar dissipation model with appropriate spray source terms. The unmixed fuel zone could be better described by introducing an equation for the conditional fuel mass fraction in this region. The diffusion flame description could be much improved by using variance and scalar dissipation rate as input parameters of a tabulated reaction rate database extracted from flamelet libraries.

## ACKNOWLEDGEMENTS

The authors acknowledge the *Groupement Scientifique Moteurs (GSM)* with *Renault SA, PSA Peugeot Citroën* and *IFP*) which supported the experimental campaign and the model development work. They would like to thank Dr. J.M. Duclos for having initiated in his previous work at *IFP* the development of the ECFM3Z combustion model.

## REFERENCES

Abraham, J., Bracco, F.V. and Reitz, R. D. (1985) Comparison of Computed and Measured Premixed Charge Engine Combustion. *Combust. Flame*, **60**, 309.

Béard, P., Colin, O. and Miche, M. (2003) Improved Modelling of DI Diesel Engines Using Sub-grid Descriptions of Spray and Combustion. *SAE Paper* 2003-01-0008.

Bilger, R.W. (1993) Conditional Moment Closure for Turbulent Reacting Flow. *Phys. Fluids*, **A 5**, 2, 436.

Bohbot, J., Zolver, M., Klahr, D. and Torres, A. (2003) Three Dimensional Modelling of Combustion in a Direct Injection Diesel Engine Using a New Unstructured Parallel Solver. *Simulation and Modeling, in Computational Science and Its Applications - ICCSA 2003*, Springer-Verlag, Berlin Heidelberg.

Boudier, P., Henriot, S., Poinsot, T. and Baritaud, T. (1992) A Model for Turbulent Flame Ignition and Propagation in Piston Engines. *24th Symposium (International) on Combustion*, The Combustion Institute.

Candel, S. and Poinsot, T. (1990) Flame Stretch and the Balance Equation for the Flame Area. *Combustion Science and Technology*, **70**, 1-15.

Chalak, Z. (1990) Modélisation du délai d'auto-inflammation dans un moteur Diesel ; validation expérimentale. *PhD Thesis*, Rouen University.

Chen, C., Bardsley, M. and Johns, R. (2000) Two-Zone Flamelet Combustion Model. *SAE Paper* 2000-01-2810.

Colin, O, Benkenida, A. and Angelberger, C. (2003) A 3D Modeling of Mixing, Ignition and Combustion Phenomena in Highly Stratified Gasoline Engines. *Oil & Gas Science and Technology, Rev. IFP*, **58**, 1, 47-62.

Colin, O., Pires da Cruz, A. and Jay, S. (2004) Detailed Chemistry Based Auto-Ignition Model Including Low Temperature Phenomena Applied to 3D Engine Calculations. *30th Symposium (International) on Combustion*, Pittsburgh, The Combustion Institute, 2649-2656.

Curran, H.J., Gaffuri, P., Pitz, W.J. and Westbrook, C.K. (1998) A Comprehensive Modeling Study of n-Heptane Oxidation. *Combust. Flame*, **114**, 149.

Dec, J.E. (2002) A Computational Study of the Effects of Low Fuel Loading and EGR on Heat Release Rates and Combustion Limits in HCCI Engines. *SAE Paper* 2002-01-1309.

Docquier, N. (2003) Experimental Investigations in an Optical HCCI Diesel Engine. About the Influence of Fresh Charge Preparation and Composition on Auto-Ignition Delays and Combustion Development. *19th International Colloquium on the Dynamics of Explosions and Reactive Systems*, Hakone, Japan, 27 July-1 August.

Duclos, J.M., Bruneaux, G. and Baritaud, T. (1996) 3D Modelling of Combustion and Pollutants in a 4Valve SI Engine: Effect of Fuel and Residuals Distribution and Spark Location. *SAE Paper* 961964.

Duclos, J.M. and Colin, O. (2001) Arc and Kernel Tracking Ignition Model for 3D Spark-Ignition Engine Calculation. *International Symposium COMODIA*.

Duclos, J.M. and Zolver, M. (1998) 3D Modeling of Intake, Injection and Combustion in a DI-SI Engine under Homogeneous and Stratified Operating Conditions. *International Symposium COMODIA*.

Gicquel, O., Darabiha, N. and Thévenin, D. (2000) Laminar Premixed Hydrogen/Air Counterflow Flame Simulations Using Flame Prolongation of ILDM with Differential Diffusion. *28st Symposium (International) on Combustion*, Pittsburgh, The Combustion Institute.

Hasse, C., Bikas, G. and Peters, N. (2000) Modeling DI Diesel Combustion using the Eulerian Particle Flamelet Model (EPFM). *SAE Paper* 2000-01-2934.

Henriot, S., Bouyssounnouse, D. and Baritaud, T. (2003) Port Fuel Injection and Combustion Simulation of a Racing Engine. *SAE Paper* 2003-01-1845.

Heywood, J.B. (1988) Pollutant Formation and Control. In: *Internal Combustion Engine Fundamentals*, McGraw-Hill, Inc.

Kleemann, A.P., Menegazzi, P., Henriot, S. and Marchal, A. (2003) Numerical Study on Knock and SI Engine by Thermally Coupling Combustion Chamber and Cooling Circuit Simulations. *SAE Paper* 2003-01-0563.

Klimenko, A. and Yu, (1990) Multicomponent Diffusion of Various Admixtures in Turbulent Flow. *Fluid Dynamics*, **25**, 327.

Kong, S.C., Han, Z. and Reitz, R.D. (1995) The Development and Application of a Diesel Ignition and Combustion Model for Multidimensional Engine Simulation. *SAE Paper* 950278.

Lafossas, F.A., Castagne, M., Dumas, J.P. and Henriot, S. (2002) Development and Validation of a Knock Model in Spark Ignition Engines Using a CFD Code. *SAE Paper* 2002-01-2701.

Marble, F.E. and Broadwell, J.E. (1977) The Coherent Flame Model of Non-Premixed Turbulent Combustion. *Projet Squid TRW-9-PU, Projet Squids Headquarters*, Chaffee Hall, Purdue University.

Martinot, S., Béard, P. and Roesler, J. (2001) Comparison and Coupling of Homogeneous Reactor and Flamelet Library Soot Modeling Approaches for Diesel Combustion. *SAE Paper* 2001-01-3684.

Peters, N. (1986) Laminar Flamelet Concepts in Turbulent Combustion. *21st Symposium (International) on Combustion*, Pittsburgh, The Combustion Institute.

Pitsch, H., Wan, Y.P. and Peters N. (1995) Numerical Investigation of Soot Formation and Oxidation under Diesel Engine Conditions. *SAE Paper* 952357.

Pitsch, H., Chen, M. and Peters, N. (1998) Unsteady Flamelet Modeling of Turbulent Hydrogen-Air Diffusion Flames. *27th Symposium (International) on Combustion*, Pittsburgh, The Combustion Institute.

Réveillé, B., Miche, M., Jay, S. and Henriot, S. (2004) Contribution of 3D CFD Tools to the Development and Understanding of Diesel Engines: Improving Today's Engines and Designing Tomorrow's Poser Units. *SIA, Le Diesel : aujourd'hui et demain*, École centrale de Lyon, 12-13th May.

Tap, F.A., Hilbert, R., Thévenin, D. and Veynante D. (2004) A Generalized Flame Surface Density Modelling Approach for the Auto-Ignition of a Turbulent Non-Premixed System. *Combust. Theory Modelling*, **8**, 1, 163-193.

Van Kalmthout, E., Veynante, D. and Candel, S. (1996) Direct Numerical Simulation Analysis of Flame Surface Density Equation in Non-premixed Turbulent Combustion. *26th Symposium (International) on Combustion*, Pittsburgh, The Combustion Institute.

Vervish, L., Hauguel, R., Domingo, P. and Rullaud, M. (2004) Three Facets of Turbulent Combustion Modelling: DNS of Premixed V-flame, LES of lifted nonpremixed flame and RANS of jet-flame. *Journal of Turbulence*, 5, 004.

Veynante, D. and Vervisch, L. (2002) Turbulent Combustion Modeling. *Progress in Energy and Combustion Science*, **28**, 93-266.

Zhang *et al.* (2004) Multidimensional HCCI Modeling Using Complex Chemistry and Transported pdf's. *30th Symposium (International) on Combustion*, Pittsburgh, The Combustion Institute.

Zolver, M., Benkenida, A., Bohbot, J., Klahr, D. and Réveillé, B. (2004) CFD Tools at IFP for HCCI Engine Simulations. *14th International Multidimensional Engine Modeling User's Group Meeting at the SAE Congress*, Detroit, Michigan, 7 March.

Zolver, M., Bohbot, J., Klahr, D. and Torres, A. (2004) An Unstructured Parallel Solver for Multi-Phase and Reactive Flows in Internal Combustion Engines. Combustion Problems. In: *Parallel Computational Fluid Dynamics*, Elsevier BV, Amsterdam.

Zolver, M., Klahr, D., Bohbot, J., Laget, O. and Torres, A. (2003) Reactive CFD in Engines with New Unstructured Parallel Solver. *Oil & Gas Science and Technology, Rev. IFP*, **58**, 1, 33-46.

*Final manuscript received in December 2004*